

A simple and accurate craniofacial midsagittal plane definition

Q16 Moshe Noam Green,^a Jonathan Michael Bloom,^b and Richard Kulbersh^a
 Detroit, Mich, and Cambridge, Mass

Introduction: In this article, we aimed to establish an ideal definition for the craniofacial midsagittal plane (MSP) by first finding an optimal “plane of best fit” and then deriving a simple approximation for clinical use that is highly accurate. **Methods:** For 60 adolescent patients, 3-dimensional coordinates of 8 central landmarks and 6 pairs of lateral landmarks were collected. Across all patients, the coplanarity of the central landmarks was compared with that of the midpoints of the lateral landmarks. The MSP of best fit was then found by minimizing the mean square distance of the 8 central landmarks to a plane. Across all patients, each possible 3-point plane was compared with the MSP of best fit with respect to both orientation and proximity. **Results:** The central landmarks were more coplanar and thus more accurate than the midpoints of the lateral pairs. The plane defined by nasion, basion, and incisive foramen was the closest to the MSP of best fit in both orientation and proximity. **Conclusions:** The nasion-basion-incisive foramen plane should be used for skull orientation and 3-dimensional cephalometric analyses because it approximates the MSP of best fit with high accuracy, avoids the use of horizontal reference planes, avoids influence from upper and midface asymmetry, uses easily identifiable relevant landmarks, and is simple to define. (Am J Orthod Dentofacial Orthop 2017; ■: ■-■)

The midsagittal plane (MSP) is the only major plane of symmetry in the craniofacial complex, and it sets the foundation for skull orientation and 3-dimensional (3D) cephalometric analyses. Skull orientation is an important first step when carrying out 3D diagnoses for the following reasons. First, it dramatically affects our ability to visually assess the skull for asymmetries. Second, if a cone-beam computed tomography (CBCT) image is being reformatted into a 2-dimensional radiograph, angular deviations foreshorten and skew the proportions of the resulting image. Finally, multiple 3D landmarks are orientation-dependent. For instance, it is not uncommon for a landmark to be defined as “the most lateral, anterior, inferior, or posterior point” on a given structure. Aside from being used for skull orientation, the MSP serves as a reference plane for both 3D cephalometric analyses and for the superimposition of radiographs from different time points.

Authors primarily use the MSP as a reference plane for skull orientation.¹⁻¹⁰ However, a true craniofacial plane of symmetry exists only as a theoretical construct, since no human is perfectly symmetric. Thus, there is wide variation among MSP definitions in the literature. Various definitions rely on other horizontal reference planes (eg, Frankfort horizontal),⁷⁻¹⁰ midpoints of lateral landmarks (eg, anterior clinoid processes, foramina spinosum, orbitale, porion, and so on),^{6,8-10} central landmarks (eg, sella, nasion, crista galli, anterior nasal spine, and so on),^{4,5} or a combination of these. It stands to reason, however, that an ideal definition of the MSP would incorporate as many relevant landmarks as possible. The purposes of this study were to (1) establish this ideal definition, to be called the MSP of best fit, and (2) derive a simple and accurate protocol for approximating it.

MATERIAL AND METHODS

Approval from the Institutional Review Board at the University of ●● was obtained. Volumetric data from Q1 CBCT radiographs acquired with the Next Generation scanner (i-CAT, Hatfield, Pa) were collected from the University of Detroit Mercy Department of Orthodontics database. A total of 60 pretreatment radiographs were Q2 selected from adolescent patients who had no prior orthodontic treatment and no obvious craniofacial anomalies. Ten patients from each of the following groups

^aSchool of Orthodontics, University of Detroit Mercy, Detroit, Mich.

^bDepartment of Mathematics, Massachusetts Institute of Technology, Cambridge, Mass.

All authors have completed and submitted the ICMJE Form for Disclosure of Potential Conflicts of Interest, and none were reported.

Address correspondence to: Moshe Noam Green, 1691 Parliament Pt, Atlanta, GA 30329; e-mail, noamgreen@gmail.com.

Submitted, April 2016; revised and accepted, December 2016.

0889-5406/\$36.00

© 2017 by the American Association of Orthodontists. All rights reserved.

<http://dx.doi.org/10.1016/j.ajodo.2016.12.025>

(designations recommended by the Food and Drug Administration¹¹ and the National Institutes of Health¹²) were randomly selected: 10 black boys (average age, 13.3 years), 10 black girls (average age, 13.2 years), 10 Hispanic boys (average age, 12.0 years), 10 Hispanic girls (average age, 12.4 years), 10 white boys (average age 12.8 years), and 10 white girls (average age, 12.1 years). The average age of all 60 patients was 12.6 years.

03 The images were obtained in DICOM format and imported into Dolphin software (version 11.7 premium; Dolphin Imaging, Chatsworth, Calif). Each DICOM image was imported into the 3D imaging tool. The volumetric image was then adjusted for segmentation and opacity to allow for adequate visualization of the anterior nasal spine and minimize scatter. The radiographs were visually oriented from the front, right, and top views using the orientation tool.

Twenty craniofacial landmarks were selected for each patient with the Dolphin digitize/measurement tool. The landmarks were categorized as either central or lateral. Central landmarks were expected to sit on the MSP (Fig 1), whereas lateral landmarks were expected to have mirror symmetry across the MSP. Although some of the 3D landmarks used in this study share names with 2-dimensional landmarks (eg, nasion, sella, basion, anterior nasal spine, posterior nasal spine, orbitale), these landmarks are fundamentally different. Although traditional cephalometric 2-dimensional landmarks display adequate reliability when used in 3D analyses, each 3D landmark has been explicitly defined for added accuracy.¹³

Eight central landmarks (Fig 1) were defined 3-dimensionally as follows.

1. Nasion (N): the most anterior aspect of the fronto-nasal suture from a sagittal view and centered mediolaterally from the axial and coronal views.^{7,10,14-16}
2. Crista galli (CG): the most posterior and inferior point of the perpendicular plate of the ethmoid bone where it joins the cribriform plate from a sagittal view and centered mediolaterally on the junction of the perpendicular plate of the ethmoid bone and the cribriform plate from the axial and coronal views.^{3,8}
3. Sella (S): the center of the space in sella turcica from a sagittal view, centered mediolaterally on the base of sella turcica from the axial and coronal views.^{7,10,14,16}
4. Basion (Ba): the middorsal point of the anterior margin of the foramen magnum on the basilar part of the occipital bone, located at the most posterior and inferior point of the basilar part of the occipital bone from a sagittal view and centered middorsally from the axial and coronal views.^{10,13,14}
5. Vomer (V): the most posterior and inferior aspect of the sulcus vomeris from a sagittal view and centered mediolaterally from the axial and coronal views.
6. Posterior nasal spine (PNS): the most posterior point of the posterior nasal spine from the sagittal and axial views. If bilateral processes are visible, their midpoint is selected.^{13,14,17}

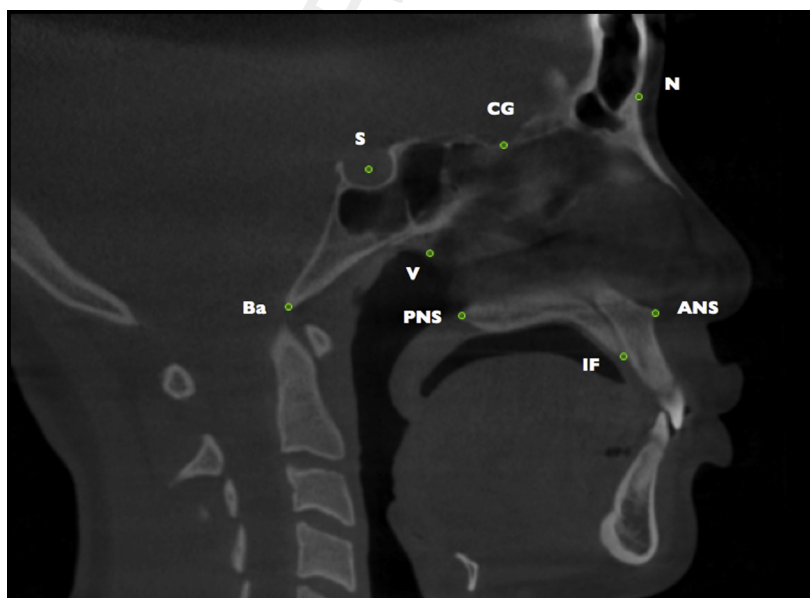


Fig 1. Sagittal CBCT slice illustrating the 8 central landmarks.

- 253
254
255
256
257
258
259
260
261
262
263
264
265
266
267
268
269
270
271
272
273
274
275
276
277
278
279
280
281
282
283
284
285
286
287
288
289
290
291
292
293
294
295
296
297
298
299
300
301
302
303
304
305
306
307
308
309
310
311
312
313
314
315
7. Incisive foramen (IF): the anteroposterior and mediolateral center of the incisive foramen as it exits the maxilla viewed from the sagittal and axial views, respectively.
 8. Anterior nasal spine (ANS): the most anterior point of the anterior nasal spine from the sagittal and axial views. If bilateral processes are visible, their midpoint is selected.^{7,8,13-17}
- Six pairs of lateral landmarks were defined as follows.
1. Zygomaticofrontal suture (ZFS): the center of the area of the axial slice of the zygomaticofrontal suture.^{10,13,15}
 2. Anterior clinoid process (ACP): the most posterior point of the anterior clinoid process when viewed sagittally and axially.^{5,8,10}
 3. Porion (Po): the superior aspect of the external auditory meatus when viewed sagittally, positioned mediolaterally where the superior epithelium tapers to its thinnest point.^{3,5,7,8,10,13-15}
 4. Foramen spinosum (FSp): the axial center of the area of the foramen spinosum at its most superior point as it joins the cranial fossa.^{10,13}
 5. Orbitale (Or): the most inferior point of the orbital sphere when oriented to the Frankfort horizontal.^{5,7,8,10,14-16}
 6. Lateral foramen magnum (LFM): the most lateral point of the foramen magnum when viewed axially, vertically centered on the most convex point of the foramen when viewed coronally.^{5,10}

The central landmarks were chosen for their ease of identification and biologic relevance. From a developmental standpoint, the cranial base sets the foundation for craniofacial development. This cartilaginous core is represented well by Ba, V, CG, and S. N, ANS, IF, and PNS represent the anterior and inferior portion of the craniofacial complex. The lateral landmarks were also chosen because of their ease of identification and to represent various regions of the skull. ZFS and Or represent the orbit, FSp and ACP represent the middle cranial fossa, Po represents the lateral extent of the skull, and LFM represents the posterior aspect of the posterior extent of the area of interest.

Landmarks of the mandible were not used since the mandible does not rigidly articulate with the rest of the skull. Because it is free to move, its development and position at the time of exposure may be subject to functional and environmental influence. Additionally, landmarks posterior to foramen magnum (eg, inion, opisthion) were not used since they are not visually relevant.

The general protocol for landmark selection included 3 steps: (1) locating the desired landmark in the sagittal

view anteroposteriorly and superoinferiorly, (2) refining the landmark position mediolaterally from the coronal and axial views, and (3) selecting the landmark from the sagittal view. The 20 landmarks were selected for each of the 60 patients by the first author. The x, y, and z coordinates of all 1200 points were exported to Excel (Microsoft, Redmond, Wash), converted to Comma Separated Value format (*.csv), and then imported into the statistical computing software R (available at www.r-project.org).

For each of the 60 adolescents, 3D coordinates of 8 central landmarks and 6 pairs of lateral landmarks were collected. The 6 midpoints of the lateral landmarks were then calculated as well. To establish an ideal definition of the MSP, the degree to which the 8 central points agree on 1 plane, compared with the 6 midpoints, was considered. To measure the coplanarity of a set of points, the following mathematical notions were used.

Let p_1, \dots, p_n be n points in 3D space. Let P be a plane. Let d_i be the (perpendicular) distance from the point p_i to the plane P . The mean absolute distance or mean absolute error (MAE) of the points with respect to the plane P is the mean of the distances. The mean square distance or mean square error (MSE) of the points with respect to the plane P is the mean of the squared distances.

$$MAE = \frac{1}{n} \sum_{i=1}^n d_i \quad MSE = \frac{1}{n} \sum_{i=1}^n d_i^2$$

Although MAE may be a more intuitive notion, MSE is more sensitive to outliers and has better mathematical properties. The plane of best fit for the points p_1, \dots, p_n is the plane P that minimizes the MSE. It is a unique plane (assuming the points are not colinear) and may be calculated using linear algebra. The plane of best fit and the resulting MAE and MSE were then computed for both the 8 central landmarks and the 6 midpoints across all patients.

Once the higher degree of central landmark coplanarity was established, the MSP of best fit using all 8 central landmarks was constructed for each patient. The 3 central landmarks whose plane most accurately approximated this MSP of best fit was then determined as follows. For each of the 56 combinations of 3 central landmarks, the plane through those 3 landmarks was compared with the MSP of best fit across all 60 patients with respect to both orientation and proximity.

For orientation, the angle between the 3-point plane and the MSP of best fit was measured. The angle between 2 planes is defined as the angle between the normal vectors (perpendicular directions) to the planes,

chosen to be between 0° and 90°. For proximity, the MSE and MAE between each 3-point plane and the remaining 5 central landmarks were measured.

Q4 In addition, 3 landmarks (N, Ba, IF) across 5 randomly selected patients were analyzed for interoperator and intraoperator reliability. To test interoperator reliability, copies of written instructions were given to 5 operators; these instructions outlined the relevant features in the Dolphin Imaging software and the protocol for landmark identification and selection. No additional guidance was given to the operators during landmark selection. For each landmark, axis, and patient (eg, N along the medio-lateral x-axis for 1 patient), the standard deviation between all 5 operators was calculated. The means (across the 5 patients) of these standard deviations were also calculated. To test intraoperator reliability, the same landmarks were identified by the first author at 2 time points 3 days apart. Similarly, the mean absolute deviations of each landmark and axis were calculated.

RESULTS

For the central landmarks, for each patient, the MSE and MAE for the 8 central points with respect to their plane of best fit were computed. Across all patients, the mean MSE was 0.17 mm², and the mean MAE was 0.32 mm. For the lateral landmarks, for each patient, the MSE and MAE for the 6 midpoints with respect to their plane of best fit were also computed. Across all patients, the mean MSE was 0.22 mm², and the mean MAE was 0.35 mm.

The mean, median, and maximum angles (across all patients) for each of the 56 triples of central landmarks were calculated (Table I). The plane defined by N-Ba-IF showed the lowest mean (0.52°), median (0.46°), and maximum (1.51°) angles across all patients relative to the 8-point MSP of best fit. Additionally, in the 5 planes with the lowest mean angle, N appeared 3 times, Ba appeared 4 times, and IF appeared 3 times. By contrast, Ba-PNS-ANS had the largest mean angle of 18.67°.

For proximity, the MSE and MAE between each 3-point plane and the remaining 5 central landmarks were measured. The mean, median, and maximum MSE and MAE (across all patients) for each of the 56 triples of central landmarks were calculated (Table II). The plane defined by N-Ba-IF showed the lowest mean MSE (0.31°), median MSE (0.24°), mean MAE (0.34°), and mean MSE (0.30°), as well as the second lowest maximum MSE (1.61°) and the third lowest maximum MAE (0.81°). S-N-IF had the lowest maximum MSE (1.51°), and CG-Ba-IF had the lowest maximum MAE (0.78°).

Table I. Mean, median, and maximum angles of 56 3-point plane definitions relative to an 8-point plane of best fit

L1	L2	L3	Mean angle (°)	Median angle (°)	Maximum angle (°)
N	Ba	IF	0.52	0.46	1.51
CG	Ba	IF	0.6	0.51	2.02
N	Ba	ANS	0.61	0.5	1.57
N	S	IF	0.69	0.54	1.58
CG	Ba	ANS	0.71	0.61	2.51
N	V	IF	0.72	0.59	1.93
N	S	ANS	0.81	0.69	2.17
N	PNS	IF	0.82	0.64	2.49
N	V	ANS	0.84	0.88	1.94
N	PNS	ANS	0.86	0.87	2.44
N	S	PNS	0.91	0.78	2.59
CG	PNS	ANS	0.91	0.86	2.36
S	Ba	ANS	0.92	0.81	2.7
S	Ba	IF	0.92	0.8	2.69
CG	PNS	IF	0.95	0.81	2.77
CG	V	IF	1.02	0.82	3.85
CG	V	ANS	1.07	0.96	3.93
N	CG	IF	1.1	0.89	4.58
CG	Ba	PNS	1.13	1	2.94
N	CG	ANS	1.2	0.96	4.61
S	Ba	PNS	1.21	1.1	2.74
S	PNS	ANS	1.24	1.03	4.24
CG	S	PNS	1.28	1.09	3.39
N	Ba	PNS	1.29	1.13	3.77
CG	S	IF	1.35	1.08	4.6
N	S	V	1.53	1.49	4.08
S	PNS	IF	1.59	1.26	6.73
N	CG	PNS	1.66	1.31	6.37
CG	S	ANS	1.72	1.41	5.51
N	S	Ba	1.76	1.4	5.11
CG	S	V	1.8	1.73	4.31
S	Ba	V	1.84	1.75	4.84
N	V	PNS	1.96	1.9	6.22
Ba	V	IF	2.02	1.49	6.63
CG	S	Ba	2.03	1.8	6.08
S	IF	ANS	2.06	1.48	7.95
CG	IF	ANS	2.12	1.5	8.07
Vo	IF	ANS	2.31	1.69	8.29
S	V	ANS	2.31	2.1	5.37
Ba	V	PNS	2.45	2.15	6.24
Vo	PNS	ANS	2.46	1.95	7.52
Ba	IF	ANS	2.7	2.02	9.38
PNS	IF	ANS	2.8	2.28	10.87
N	CG	V	2.83	2.28	12.56
CG	Vo	PNS	2.9	2.22	32.33
N	IF	ANS	2.96	2.17	13.61
Ba	V	ANS	3.11	2.45	13.84
Vo	PNS	IF	3.19	2.69	15.06
CG	Ba	V	3.21	2.75	15.25
S	Vo	IF	4.16	2.76	80.46
N	CG	Ba	4.75	3.08	23.96
N	Ba	V	6.88	2.96	67.87
Ba	PNS	IF	14.09	8.82	86.04
N	CG	S	17.87	10.86	79.27
S	V	PNS	18.44	12.55	79.33
Ba	PNS	ANS	18.67	11.4	82.75

L, ...

Table II. Mean, median, and maximum MSE and MAE of 56 MSP definitions relative to the other 8 central landmarks

<i>L1</i>	<i>L2</i>	<i>L3</i>	<i>Mean MSE (mm)</i>	<i>Median MSE (mm)</i>	<i>Maximum MSE (mm)</i>	<i>Mean MAE (mm)</i>	<i>Median MAE (mm)</i>	<i>Maximum MAE (mm)</i>
N	Ba	IF	0.31	0.24	1.54	0.34	0.3	0.81
CG	Ba	IF	0.33	0.24	1.61	0.34	0.33	0.78
N	Ba	ANS	0.34	0.27	1.55	0.36	0.33	0.81
CG	Ba	ANS	0.35	0.25	1.62	0.36	0.33	0.85
N	S	IF	0.42	0.28	1.51	0.39	0.34	0.81
N	V	IF	0.43	0.34	1.73	0.4	0.37	0.87
N	V	ANS	0.47	0.34	1.7	0.41	0.38	0.87
S	Ba	ANS	0.47	0.32	1.83	0.42	0.38	0.8
N	S	PNS	0.49	0.36	2.45	0.42	0.38	0.83
S	Ba	IF	0.5	0.32	2	0.42	0.39	0.85
CG	PNS	ANS	0.5	0.37	2.32	0.43	0.37	1.06
N	PNS	ANS	0.55	0.39	3.82	0.44	0.39	1.33
N	S	ANS	0.56	0.35	2.04	0.45	0.39	1.02
CG	V	ANS	0.56	0.41	2.39	0.45	0.43	1.05
N	PNS	IF	0.56	0.36	3.48	0.44	0.39	1.27
CG	PNS	IF	0.58	0.39	2.87	0.46	0.41	1.22
CG	V	IF	0.59	0.39	3.31	0.45	0.43	1.2
CG	Ba	PNS	0.67	0.46	2.65	0.49	0.45	1.14
S	PNS	ANS	0.68	0.42	3.9	0.48	0.43	1.28
N	Ba	PNS	0.71	0.47	2.71	0.5	0.45	1.24
CG	S	PNS	0.9	0.46	4.76	0.57	0.48	1.61
S	Ba	PNS	0.91	0.6	3.5	0.57	0.52	1.35
CG	S	IF	0.91	0.53	6.79	0.57	0.49	1.82
N	S	V	1.01	0.78	3.47	0.61	0.57	1.24
N	CG	IF	1.13	0.53	10.02	0.59	0.45	2.16
S	PNS	IF	1.14	0.59	10.26	0.61	0.52	2.23
N	CG	ANS	1.3	0.58	11.89	0.64	0.49	2.4
N	CG	PNS	1.31	0.63	10.62	0.67	0.56	2.39
N	V	PNS	1.38	0.89	7.66	0.72	0.65	2.04
CG	S	ANS	1.38	0.67	9.42	0.7	0.52	2.17
CG	S	V	1.45	0.92	7.73	0.73	0.64	1.98
S	V	ANS	1.49	1.14	5.53	0.74	0.72	1.55
N	S	Ba	1.57	0.88	8.65	0.71	0.62	2.08
S	IF	ANS	1.6	0.74	12.77	0.74	0.58	2.56
Ba	V	IF	1.82	0.77	12.17	0.74	0.57	2.32
V	IF	ANS	1.83	0.9	13.03	0.79	0.68	2.56
V	PNS	ANS	1.87	1.06	11.24	0.81	0.72	2.32
S	Ba	V	2.01	1.04	13.76	0.84	0.76	2.73
Ba	V	PNS	2.14	1.16	11.35	0.88	0.75	2.3
CG	S	Ba	2.35	1.16	15.32	0.87	0.76	2.69
CG	IF	ANS	2.95	0.98	22.23	0.97	0.71	3.54
Ba	V	ANS	2.97	1.25	28.62	0.96	0.76	3.76
N	CG	V	3.08	1.51	24.5	0.99	0.83	3.37
Ba	IF	ANS	3.16	1.34	20.7	1	0.82	3.13
PNS	IF	ANS	3.45	1.55	36.6	1.04	0.79	4.43
V	PNS	IF	4.09	1.7	51.48	1.1	0.87	4.95
CG	Ba	V	4.66	1.77	36.73	1.15	0.86	4.09
CG	V	PNS	5.93	1.34	203.92	1.14	0.85	11.13
N	CG	Ba	10.66	2.71	130.93	1.62	1.07	7.99
N	IF	ANS	10.77	3.26	121.15	1.76	1.34	8.39
S	V	IF	13.51	1.83	660.51	1.23	0.92	18.33
N	Ba	V	24.21	2.2	570.64	2.09	1.03	16.62
Ba	PNS	IF	93.42	20.85	925.94	4.58	3.04	20.95
Ba	PNS	ANS	127.19	26.22	979.71	5.6	3.49	21.87
S	V	PNS	173.21	50.79	1270.45	7.5	5.41	26.98
N	CG	S	173.49	40.54	1012.68	6.99	4.82	24.01

L, ●●●.

Table III. Interoperator mean standard deviations

	<i>x</i> (mediolateral) (mm)	<i>y</i> (superoinferior) (mm)	<i>z</i> (anteroposterior) (mm)
N	0.54*	0.41	0.2
Ba	0.41	0.36	0.41
IF	0.31	0.65*	0.26
ANS	0.42	0.34	1.04*

*... .

Table IV. Intraoperator mean absolute deviations

	<i>x</i> (mediolateral) (mm)	<i>y</i> (superoinferior) (mm)	<i>z</i> (anteroposterior) (mm)
N	0.18	0.18	0.22
Ba	0.14	0.12	0.26
IF	0.14	0.34*	0.28
ANS	0.2	0.3	0.32*

*... .

The interoperator reliability mean standard deviations (Table III) and the intraoperator reliability mean absolute deviations (Table IV) were calculated. N had the greatest interoperator mediolateral deviation with a mean standard deviation of 0.54 mm, followed by Ba (0.41 mm) and IF (0.31 mm). N also had the greatest intraoperator mediolateral deviation with a mean absolute deviation of 0.18 mm, followed by Ba and IF that were both 0.14 mm. IF showed the greatest superoinferior deviation with an interoperator mean standard deviation of 0.65 mm and an intraoperator mean absolute deviation of 0.34 mm.

DISCUSSION

Both the mean MSE and mean MAE were smaller for the central landmarks than for the midpoints of lateral landmarks. In other words, the central landmarks agreed on a MSP more than did the midpoints of the lateral landmarks and are thus more accurate when defining MSP. This holds true even though there were more central landmarks (8) than midpoints of lateral landmarks (6).

The mean MSE and MAE of a 3-point plane are equal to 0 since a plane can be made to go through the 3 points exactly. If a fourth point were added, the mean MAE would be equal to the distance of that landmark to the 3-point plane divided by 4. As points are added, the MAE and MSE are expected to increase. We would thus expect the MSE and MAE to be higher for the 8 central points than for the 6 midpoints, since fewer points are easier to fit with a plane. Because there are more central points than midpoints, the fact that the mean MSE and mean MAE were lower for the central points indicates that the central points were far more coplanar. Furthermore, central landmarks are easier to identify and simpler to use when defining a plane, making them more suitable for clinical use. For these reasons, the MSP of best fit was defined with respect to the 8 central landmarks.

The plane defined by N-Ba-IF showed the lowest mean, median, and maximum angles across all patients relative to the 8-point plane of best fit. Ba-PNS-ANS defined the plane definition with the largest mean

angle. This is not surprising, since a triangle formed by N-Ba-IF has a large area and is spread apart maximally, whereas a triangle formed by Ba-PNS-ANS has a small area and is quite flat. Ba, PNS, and ANS are roughly collinear. The expected value of the square of the angle between the normal vectors is proportional to $(1/a^2 + 1/b^2 + 1/c^2)$ where a, b, and c are the 3 heights of a triangle as calculated by the distance of each vertex to its opposite edge (Fig 2). Simply stated, the 3 landmarks used to define a plane should form a triangle that has a large area and is balanced, not too narrow in any dimension. The same plane definition, N-Ba-IF, showed the lowest mean and median MSE and MAE as well as the second lowest maximum MSE and third lowest maximum MAE. This demonstrates that the N-Ba-IF is not simply parallel to the plane of best fit but significantly close to it as well.

With regard to interoperator and intraoperator reliability, the most significant of the 3 axes is the mediolateral (x) axis, since mediolateral deviations have the greatest impact on the angulation of the resulting plane. The interoperator and intraoperator mediolateral deviations of IF were minimal; this supports use as the anteroinferior determinant of the 3-point MSP definition. Although IF showed the greatest superoinferior variation, deviation along this axis leads to minimal rotation of the plane. For both reliability tests, N showed the greatest mediolateral variation. This is of little consequence for 2 reasons. First, much like the other landmarks, the actual degree of variation is minimal (mean standard deviation, 0.54 mm). Second, N is at a significant distance from the centroid of the 8 landmarks; this gives the plane adequate stability to resist rotation.

Although Ba sits on a curved structure, it performed well as a 3D landmark in all 3 planes of space and displayed little mediolateral deviation for both interoperator reliability (0.41 mm mean standard deviation) and intraoperator reliability (0.14 mm mean absolute deviation). This correlates well with other reliability studies that identified Ba as a suitable 3D landmark.¹⁴ Furthermore, even though Ba sits in the posterior cranial fossa, the N-Ba-IF plane was closer on average to the remaining 5 landmarks (CG, S, V, PNS, ANS) than any other

694
695
696
697
698
699
700
701
702
703
704
705
706
707
708
709
710
711
712
713
714
715
716
717
718
719
720
721
722
723
724
725
726
727
728
729
730
731
732
733
734
735
736
737
738
739
740
741
742
743
744
745
746
747
748
749
750
751
752
753
754
755
756

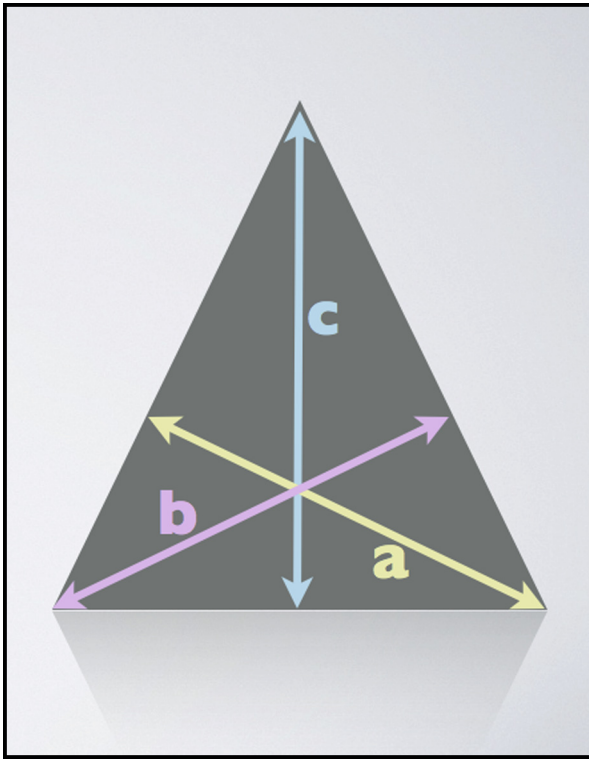


Fig 2. The expected value of the square of the angle between the normal vectors of the 3-point plane and the plane of best fit is proportional to $(1/a^2 + 1/b^2 + 1/c^2)$ where a, b, and c are the 3 heights of a triangle as calculated by the distance of each vertex to its opposite edge. It stands to reason that a 3-point plane whose 3 landmarks form a large and broad triangle is a better approximation for the plane of best fit.

plane definition. This means that Ba correlates well with the other more anterior landmarks.

A number of MSP definitions have been proposed and used in the literature.¹⁻¹⁰ We suggest the following classification system for MSP definitions as determined by the reference planes and landmarks used.

1. Type 1: planes defined as passing through 3 central structures.
2. Type 2: planes defined as passing through 3 structures, at least 1 of which is the midpoint of 2 lateral structures.
3. Type 3: planes defined as perpendicular to a different plane, passing through 2 other central structures.
4. Type 4: planes defined as perpendicular to a different plane, passing through 2 other structures, at least 1 of which is the midpoint of 2 lateral structures.

5. Type 5: other plane definitions.

To better clarify the advantages and disadvantages of different MSP definitions, 6 criteria of an ideal definition have been identified below.

1. The plane should use only central landmarks because they have a higher degree of coplanarity than do lateral landmarks. Furthermore, using mid-points of lateral landmarks is time consuming and not as practical for clinical use.
2. The plane should not use a horizontal reference plane. The horizontal plane defines the roll orientation of the MSP; this is problematic since it assumes vertical symmetry of the horizontal plane reference landmarks.
3. The plane should have landmarks that are spread apart maximally (forming a triangle that is balanced with a large area) to increase stability.
4. The plane should be formed using easily identifiable landmarks and be simple to calculate.
5. The plane should not be influenced by asymmetries of the upper ●●● and midface.
6. The plane should not use landmarks that are irrelevant to the area of diagnostic interest (posterior to foramen magnum and mandible).

Seven craniofacial MSP definitions found in the literature were described, classified, and assessed (Table V) according to the 6 criteria detailed above. Both type 3 and type 4 planes use horizontal reference planes to determine the roll orientation of the MSP.⁷⁻¹⁰ This is problematic since the horizontal reference planes are defined using lateral structures (eg, Po or Or). Any vertical asymmetry of these landmarks skews the roll orientation of the MSP. Type 2 and type 4 MSP definitions use lateral landmarks; as demonstrated earlier, these are inherently less reliable.^{6,8-10} Although a number of acceptable type 1 MSP definitions have been suggested, some use irrelevant landmarks (eg, opisthion),⁴ and others simply are not as stable as the N-Ba-IF plane.⁵

For the sake of completion, we have recommended a definition for pitch orientation as it relates to the Frankfurt horizontal and takes into account both Po and Or landmarks and avoids an effect on roll orientation (since roll and yaw have already been established by N-Ba-IF). This can be achieved by finding the point of intersection between the line connecting both Po landmarks and the MSP and the equivalent point for the Or landmarks. The skull can then be oriented so that these 2 points of intersection are parallel with the z-axis (anteroposterior).

Although the mathematical evidence supporting the N-Ba-IF plane is compelling and logical, the

Table V. Categorization and analysis of other MSP definitions

<i>Authors</i>	<i>Description of plane definition used</i>	<i>Plane type</i>	<i>Satisfied criteria</i>	<i>Unsatisfied criteria</i>
Hwang et al ³	Plane passing through opisthion, superior extent crista galli, and anterior nasal spine	Type 1	1, 2, 3, 4, 5	6
Tuncer et al ⁴	Plane passing through sella, nasion and anterior nasal spine	Type 1	1, 2, 3, 4, 5, 6	Although this plane exhibits all specified features of an ideal MSP, several other planes showed closer angular and proximal relationships to the MSP of best fit.
Damstra et al ⁵	Plane passing through nasion, the midpoint between the anterior clinoid processes, and the midpoint between the most lateral points on the foramen magnum	Type 2	2, 5, 6	1, 3*, 4 *These 3 landmarks form a relatively narrow and unstable triangle.
Proffit and White ⁶	Plane passing through sella and nasion, perpendicular to the Frankfort horizontal plane (passing through right and left orbitale and the midpoint of right and left porion)	Type 3	3, 6	1, 2, 4, 5
Yáñez-Vico et al ⁷	Plane passing through midpoint of foramina spinosum (ELSA) and middorsal point of foramen magnum (MDFM) perpendicular to a horizontal plane (bilateral superolateral border of external auditory meatus (SLEAM) and the ELSA)	Type 4	6	1, 2, 3*, 4 [†] , 5 [‡] *ELSA and MDFM are relatively close together and have low resistance to errors in yaw orientation. †ELSA has been shown to be difficult to identify in CBCT images. ⁴ ‡Vertical asymmetry of SLEAM landmarks will affect roll orientation of MSP.
Back et al ⁸ ; Kwon et al ⁹	Plane passing through most superior point of crista galli and midpoint between the 2 anterior clinoid processes, perpendicular to Frankfort horizontal plane (defined by left orbitale, right porion, and left porion)	Type 4	6	1, 2, 3*, 4, 5 [†] *Crista galli and anterior clinoid processes are only moderately spread apart and have low resistance to errors in yaw orientation. †Vertical asymmetry of porion landmarks will affect roll orientation of MSP.
Damstra et al ¹⁰	3-dimensional comparison of morphometric and conventional cephalometric MSPs for craniofacial asymmetry	Type 5	2	4*, 5 [†] *Requires additional training and software and could be more costly, limiting practical clinical use. †Relies on external landmarks of superior aspect of orbits. Using this definition in cases of orbital asymmetry will lead to misdiagnosis of the rest of the craniofacial complex and will make diagnosis of orbital asymmetry impossible.

definition is new and has not been widely used clinically. The clinical effectiveness of the plane could be validated when used as a reference plane for

3D cephalometric analyses of asymmetry. Future studies could involve establishing norms for analyses of asymmetry and validating diagnosed

asymmetries with visual diagnosis. Furthermore, additional research can validate these findings with both adult patients and patients with gross facial imbalances.

CONCLUSIONS

1. Central landmarks of the skull tend to agree on a MSP better than lateral landmarks as indicated by their higher degree of coplanarity (flatness) and are thus more suitable for use in defining the MSP.
2. The plane passing through N, Ba, and IF was the most stable and reliable craniofacial MSP definition, showing the smallest angular deviation from and the closest proximity to the MSP of best fit using all 8 central landmarks across all 60 patients.
3. The N-Ba-IF plane satisfies the 6 suggested criteria of an ideal MSP definition.
4. The N-Ba-IF definition of MSP is recommended for skull orientation and 3D cephalometric analysis.

REFERENCES

1. Lagravère MO, Major PW, Carey J. Sensitivity analysis for plane orientation in three-dimensional cephalometric analysis based on superimposition of serial cone beam computed tomography images. *Dentomaxillofac Radiol* 2010;39:400-8.
2. Hwang JJ, Kim KD, Park H, Park CS, Jeong HG. Factors influencing superimposition error of 3D cephalometric landmarks by plane orientation method using 4 reference points: 4 point superimposition error regression model. *PLoS One* 2014;9:e110665.
3. Hwang HS, Hwang CH, Lee KH, Kang BC. Maxillofacial 3-dimensional image analysis for the diagnosis of facial asymmetry. *Am J Orthod Dentofacial Orthop* 2006;130:779-85.
4. Tuncer BB, Ataç MS, Yüksel S. A case report comparing 3-D evaluation in the diagnosis and treatment planning of hemimandibular hyperplasia with conventional radiography. *J Craniomaxillofac Surg* 2009;37:312-9.
5. Damstra J, Oosterkamp BC, Jansma J, Ren Y. Combined 3-dimensional and mirror-image analysis for the diagnosis of asymmetry. *Am J Orthod Dentofacial Orthop* 2011;140:886-94.
6. Proffit WR, White RP. *Surgical-orthodontic treatment: dentofacial asymmetry*. St Louis: Mosby-Year Book; 1991.
7. Yáñez-Vico RM, Iglesias-Linares A, Torres-Lagares D, Gutiérrez-Pérez JL, Solano-Reina E. Three-dimensional evaluation of craniofacial asymmetry: an analysis using computed tomography. *Clin Oral Investig* 2010;15:729-36.
8. Baek SH, Cho IS, Chang YI, Kim MJ. Skeletodental factors affecting chin point deviation in female patients with Class III malocclusion and facial asymmetry: a three-dimensional analysis using computed tomography. *Oral Surg Oral Med Oral Pathol Oral Radiol Endod* 2007;104:628-39.
9. Kwon TG, Park HS, Ryoo HM, Lee SH. A comparison of craniofacial morphology in patients with and without facial asymmetry—a three-dimensional analysis with computed tomography. *Int J Oral Maxillofac Surg* 2006;35:43-8.
10. Damstra J, Fourie Z, Wit MD, Ren Y. A three-dimensional comparison of a morphometric and conventional cephalometric midsagittal planes for craniofacial asymmetry. *Clin Oral Investig* 2011;16:285-94.
11. Collection of race and ethnicity data in clinical trials. Available at: <http://www.fda.gov/regulatoryinformation/guidances/ucm126340.htm>. Accessed September 8, 2016.
12. NOT-OD-15-089: racial and ethnic categories and definitions for NIH diversity programs and for other reporting purposes. US National Library of Medicine. Available at: <http://grants.nih.gov/grants/guide/notice-files/not-od-15-089.html#sthash.srd3jjba.dpuf>. <http://grants.nih.gov/grants/guide/notice-files/not-od-15-089.html>. Accessed September 8, 2016.
13. Lagravère MO, Gordon JM, Guedes IH, Flores-Mir C, Carey JP, Heo G, et al. Reliability of traditional cephalometric landmarks as seen in three-dimensional analysis in maxillary expansion treatments. *Angle Orthod* 2009;79:1047-56.
14. Damstra J, Fourie Z, Huddleston Slater JJ, Ren Y. Reliability and the smallest detectable difference of measurements on 3-dimensional cone-beam computed tomography images. *Am J Orthod Dentofacial Orthop* 2011;140:e107-14.
15. Olmez H, Gorgulu S, Akin E, Bengi AO, Tekdemir I, Ors F. Measurement accuracy of a computer-assisted three-dimensional analysis and a conventional two-dimensional method. *Angle Orthod* 2011;81:375-82.
16. Oliveira AE, Cevidanes LH, Phillips C, Motta A, Burke B, Tyndall D. Observer reliability of three-dimensional cephalometric landmark identification on cone-beam computerized tomography. *Oral Surg Oral Med Oral Pathol Oral Radiol Endod* 2009;107:256-65.
17. Gribel BF, Gribel MN, Frazão DC, McNamara JA, Manzi FR. Accuracy and reliability of craniometric measurements on lateral cephalometry and 3D measurements on CBCT scans. *Angle Orthod* 2011;81:26-35.